Three phase PWM rectifier with integrated battery for automotive applications

Shetty, Akshatha; Fernandes, B. G.; Ojo, Joseph Olorunfemi; Ferreira, J. A.

DOI
10.1109/IAS.2018.8544681

Publication date
2018

Document Version
Final published version

Published in
2018 IEEE Industry Applications Society Annual Meeting, IAS 2018

Three Phase PWM Rectifier with Integrated Battery for Automotive Applications

Akshatha Shetty, B. G. Fernandes
Department of Electrical Engineering
Indian Institute of Technology Bombay
Mumbai, India 400076
Email: akshatha@iitb.ac.in

Joseph Olorunfemi Ojo
Department of Electrical and Computer Engineering
Tannesse Technological University
Cookeville, TN 3805, U.S.A
Email: jojo@tntech.edu

J. A. Ferreira
Delft University of Technology
The Netherlands
Email: j.a.ferreira@tudelft.nl

***Abstract*—Vehicle ergonomics is one of the most important objectives for automotive applications. Reducing the size and weight is a prime concern for mobility. A novel unified converter with battery integration is proposed as an alternative to the existing power train configuration for hybrid electric vehicles. The power train has three phase PWM rectifier at the output of the alternator with battery connected to the neutral of the induction generator stator. With the proposed topology, vehicle size and weight can be reduced considerably. The topology is analysed for its control and performance specifications. Simulation studies are carried out in MATLAB/SIMULINK and results are presented.**

***Index Terms*—Multifrequency power, superposed ac-dc, PWM rectifiers, unified ac-dc.**

I. Introduction

RAPIDLY depleting fossil fuels like coal, oil and natural gas pose a real challenge in meeting the energy requirement for mobility. For sustained transportation, it is important to find an alternative source of energy which is clean, reliable and inexpensive along with fuel efficient technology. This motivation has led to tremondous research in the field of advanced vehicular technology. These advanced vehicles are classified into Battery Electric Vehicle (BEV), Fuel Cell Electric Vehicle (FCEV), and Fuel Cell Hybrid Electric Vehicle (FCHEV). Hybrid Electric Vehicles (HEV) have an internal Combustion Engine (ICE) and Electric Motor (EM), which make the vehicle fuel efficient. Large Energy Storage Systems (ESS) such as a battery or ultracapacitors are used by full hybrid electric vehicles. The rating of EM used in full HEV is 50kW/330V [1]. Four types of technology used for this are; series full-HEV, parallel full-HEV, series-parallel full-HEV and complex full-HEV [1]–[3].

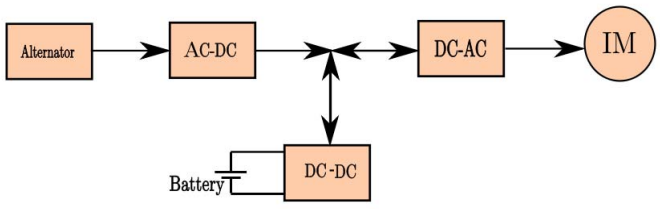

Fig. 1. Power train arrangement for a series HEV

Similar to BEV, EM is used for main propulsion in series full HEVs. An example of series full-HEV is Chevrolet Volt Series. Full-HEVs is configured with a high power ICE generator/fuel cells and an Energy Storage System (ESS). The requirement of ESS are twofold, to improve the dynamic performance of the power train and to recover the vehicle kinetic energy while braking [1]–[3]. The typical power train arrangement is as shown in the Fig. 1 [1]–[3]. One of the most common converters used in the hybrid systems is AC/DC/DC converter since two different power sources can be connected [4]. The alternator supplies the constant power to the load and the battery is connected to absorb the power fluctuations during peak energy demands. However, this increases the mass of the vehicle, which raises the power demand and thus the fuel consumption. Thus, advantages of adding an ESS to the powertrain can also become a drawback due to this effect [4]. The complexity and cost of such systems is also one of the drawbacks for hybridisation.

In order to address the above issues, numerous topologies are proposed which can reduce the size and weight of the vehicle. There is very little literature on unified converters. The unified converters – single converter used to process both ac and dc power. In [4]–[6] authors have proposed reactor free boost converter for BEV. Here battery being the single source of power, connected to the stator neutral of the motor, the converter which is driving the motor is used as the boost converter for the battery. The leakage inductance of the motor is used as the boost inductance, thereby reducing its size and weight. In this paper a similar approach is followed and an alternate topology for the existing power train arrangement in hybrid electric vehicles is proposed. The proposed topology uses a single converter to process the power from two different sources of different frequencies (generator and ESS). A battery is connected in the stator neutral of an induction generator. The PWM rectifier is used to convert generator ac voltage to dc and acts as a boost converter for the battery while maintaining the output dc voltage.

II. Three phase PWM rectifier with battery Integration

The proposed topology is as shown in Figs. 2 and 3. An existence function represents the turn-on and turn-off sequences

978-1-5386-4536-9/18/$31.00 © 2018 IEEE

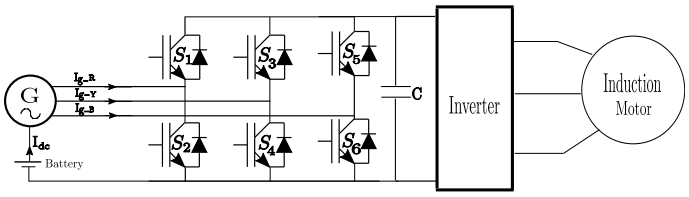

Fig. 2. PWM rectifier with battery integration

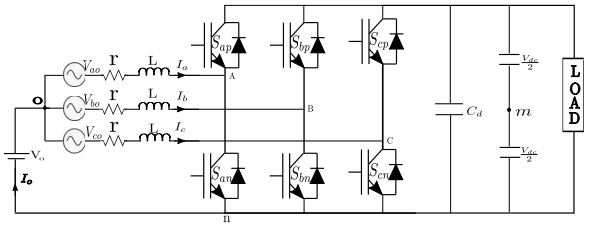

Fig. 3. PWM rectifier with battery integration

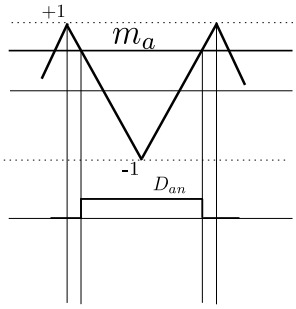

Fig. 4. Modulation

of a switching device. This function, Sij =1 when it is turned on and Sij =0, when it is off; where i represents the phase to which the device is connected and j signifies top (p) and bottom (n) device of the converter leg.

V_{ao}, V_{bo} & V_{co} are balanced ; $I_a = I_{aa} \pm I_{oo}$, $I_b = I_{bb} \pm I_{oo}$, $I_c = I_{cc} \pm I_{oo}$; $I_a + I_b + I_c = \pm I_o$ and $I_{oo} = \pm \frac{I_o}{3}$

'+' denotes charging
'-' denotes discharging

$$V_{ao} = rI_a + LpI_a + \frac{V_{dc}}{2}S_{ap} - \frac{V_{dc}}{2}S_{an} + V_{mo}$$
$$V_{bo} = rI_b + LpI_b + \frac{V_{dc}}{2}S_{bp} - \frac{V_{dc}}{2}S_{bn} + V_{mo}$$
$$V_{co} = rI_c + LpI_c + \frac{V_{dc}}{2}S_{cp} - \frac{V_{dc}}{2}S_{cn} + V_{mo} \quad (1)$$

Where, $p = \frac{d}{dt}$
Substituting $V_{mo} = \frac{V_{dc}}{2} - V_o$ and $S_{an} = 1 - S_{ap}$

$$V_{ao} + V_o = rI_a + LpI_a + \frac{V_{dc}}{2}(2S_{ap} - 1) + \frac{V_{dc}}{2}$$
$$V_{bo} + V_o = rI_b + LpI_b + \frac{V_{dc}}{2}(2S_{bp} - 1) + \frac{V_{dc}}{2}$$

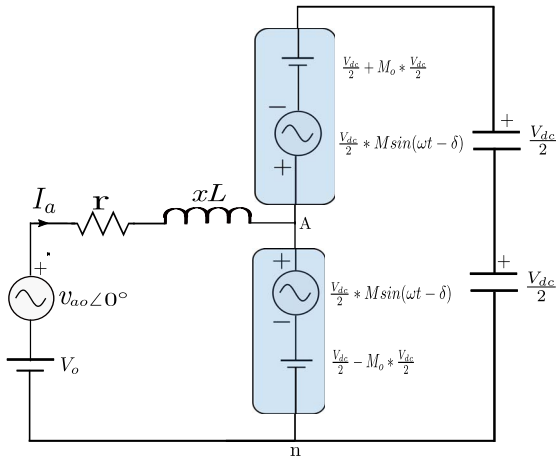

Fig. 5. Equivalent circuit of PWM rectifier

$$V_{co} + V_o = rI_c + LpI_c + \frac{V_{dc}}{2}(2S_{cp} - 1) + \frac{V_{dc}}{2} \quad (2)$$

The modulating wave is of the form

$$m_a = M_o - Msin\omega t$$
$$m_b = M_o - Msin(\omega t - 120°)$$
$$m_c = M_o - Msin(\omega t - 240°) \quad (3)$$

substituting $S_{ip} = 0.5[1 - m_i]$ [7], where, i=a,b,c in Eq.(2) we get,

$$V_{ao} + V_o = rI_a + LpI_a + \frac{V_{dc}}{2}Msin(\omega t - \delta) - M_o\frac{V_{dc}}{2} + \frac{V_{dc}}{2}$$
$$V_{bo} + V_o = rI_b + LpI_b + \frac{V_{dc}}{2}Msin(\omega t - 120° - \delta) - M_o\frac{V_{dc}}{2} + \frac{V_{dc}}{2}$$
$$V_{co} + V_o = rI_c + LpI_c + \frac{V_{dc}}{2}Msin(\omega t - 120° - \delta) - M_o\frac{V_{dc}}{2} + \frac{V_{dc}}{2} \quad (4)$$

The per phase ac current for 'a' phase is given by,

$$I_{aa} = \frac{V_{ao}\angle 0° - V_2\angle \delta°}{j\omega L}$$

where $V_2 = \frac{MV_{dc}}{2\sqrt{2}}$. The per phase dc current is given by

$$I_{oo} = \frac{V_o - (\frac{V_{dc}}{2} - M_o\frac{V_{dc}}{2})}{r}$$

III. Neutral current ripple

Since the battery is connected to the neutral, the battery current ripple must be maintained low along with the line current ripple. In case of a PWM converter, the PWM scheme plays an important role in determining the current distortion. Therefore, a suitable PWM scheme is necessary to minimise the current ripple.

978-1-5386-4536-9/18/$31.00 © 2018 IEEE

$$S_{an} = 0.5[1+m_a] + \underbrace{\frac{2}{\pi}\sum_{m=1}^{\infty}\frac{J_o}{m}(m\frac{\pi}{2}M)sin(\frac{\pi}{2}M)cos[m(\omega_c t+\theta_c)]}_{Carrier} + \underbrace{\frac{2}{\pi}\sum_{m=1}^{\infty}\sum_{n=-\infty}^{\infty}\frac{J_n}{m}(m\frac{\pi}{2}M)sin[(m+n)\frac{\pi}{2}]cos[m(\omega_c t+\theta_c)+n(\omega_o t+\theta_o)]}_{Side-Band-Harmonics} \quad (5)$$

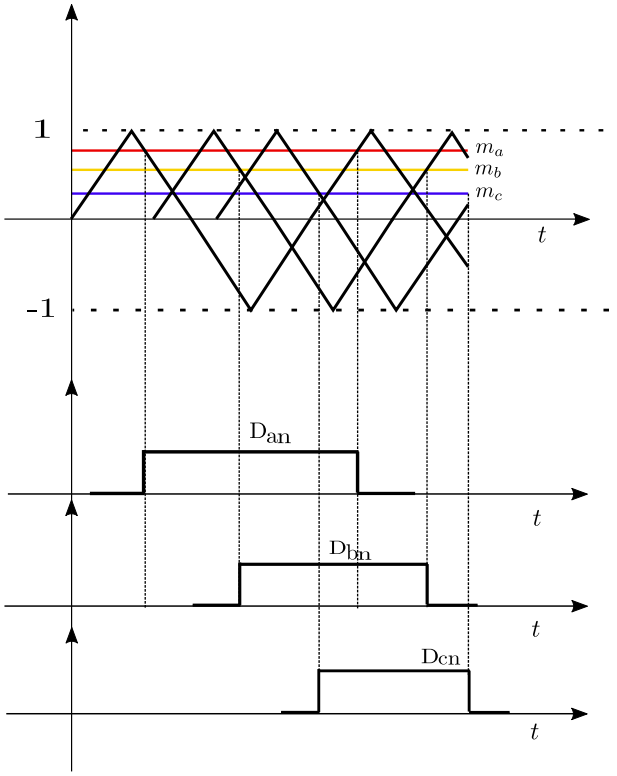

Fig. 6. PS-SPWM scheme

A. Line and Neutral Current Ripple Analysis with Single Carrier and Phase Shifted Carrier

Substituting $S_{ap} = 1 - S_{an}$ in equation (1),

$$V_{ao} + V_o = rI_a + LpI_a + \underbrace{\frac{V_{dc}}{2}(1-2S_{an}) + \frac{V_{dc}}{2}}_{v_{An}}$$

Substituting the Fourier series expansion for the switching function as given in Eq.(5) [7], the instantaneous pole voltage v_{An} contains averaged value V_{An} and switching frequency ripple component $\widetilde{v_{An}}$. The ripple voltage $\widetilde{v_{An}}$ will introduce ripple component in the line current I_a. So the ripple component in the line current can be written as

$$\widetilde{i_a} = -\frac{1}{L}\int \widetilde{v_{An}}dt$$

Conventional Sine-triangle PWM (SPWM) scheme is the simplest and widely used PWM technique for three-phase PWM converters. With this modulation scheme, in the equation (5) the term θ_c is same for all three phases. The neutral current ripple can be written as

$$\widetilde{i_N} = \widetilde{i_a} + \widetilde{i_b} + \widetilde{i_c} \quad (6)$$

It is clear from the equations (5) and (6) that, with SPWM, the current ripple in each phase adds, therefore peak-to-peak ripple in the neutral current is higher than the peak-to-peak ripple in any of the three line currents. From (5) it is also clear that, by introducing suitable phase shifts between three phase line current ripple at carrier frequency, the neutral current can be reduced considerably. This can be achieved by using three Phase Shifted carrier SPWM method (PS-SPWM). In this scheme, the carrier is shifted by 120° apart. With the battery connected in the neutral, the line current ripple is only dependant on the corresponding phase pole voltage. So the line current THD in SPWM and PS-PWM are comparable.

IV. Current Controller Structure

The proposed topology utilises a single converter to extract the power from two sources of different frequencies. The converter acts as a PWM rectifier and a current controlled interleaved boost converter simultaneously. Due to this multifunctionality, the input current is superimposed ac dc in nature (unified ac-dc). The controller needs to track unified ac-dc current closely. The appropriate controller design is carried out considering a trade-off between cost, complexity and output waveform quality. For three phase current control, synchronous PI controller is commonly used [8]. With the addition of one more PI controller, the same scheme can be extended to control the neutral dc current. Another alternative method used in three phase current control is the PR (Proportional+Resonant) control [8]. The PR controller has infinite gain at the tuned frequency. So it can track only signal of a single frequency for which PR controller is tuned.

$$G_{PR}(s) = k_p + \frac{k_r s}{s^2+\omega_o^2} \quad (7)$$

The transfer function of an ideal PR controller is given by Eq. (7). The steady state error can be reduced to zero by using an ideal PR controller with infinite gain at the tuned frequency. However due to practical limitations an ideal PR controller is often approximated as [9]

$$G_{PR}(s) = k_p + \frac{2k_r\omega_c s}{s^2+2\omega_c s+\omega_o^2}$$

The value of ω_c is selected between 5-15 rad/s [10]. Tracking unified ac dc current using the PR controller, the 'PR' term will track the sinusoidal signal of tuned frequency 'ω_o' and only the proportional term will try to track the dc component. Since only 'P' term is controlling the dc current there always exists a finite steady state error. To avoid this steady state error an integral term has to be combined with PR. With PIR it is possible to control both ac and dc current. With the use

978-1-5386-4536-9/18/$31.00 © 2018 IEEE

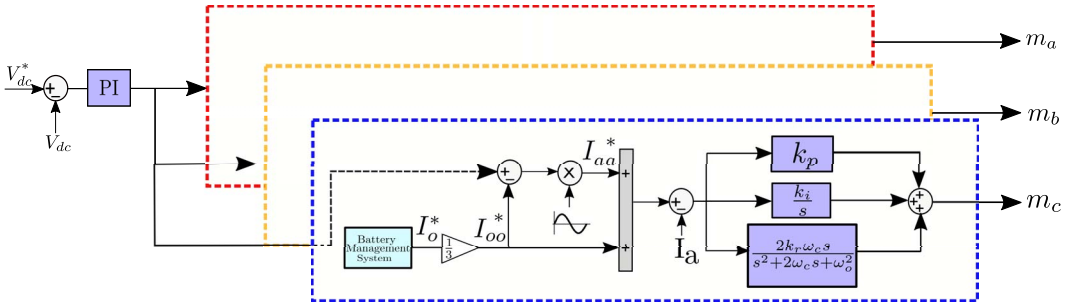

Fig. 7. Control block diagram for PWM rectifier and dc-dc boost converter

of PIR control, the dc component in each phase is controlled independently without segregating the ac and dc components in the measured line currents. This method also avoids coordinate transformations from abc to dq in order to have the currents in synchronous frame. The transfer function of PIR control can be written as

$$G_{PIR}(s) = k_p + \frac{2k_r\omega_c s}{s^2 + 2\omega_c s + \omega_o^2} + \frac{k_i}{s}$$

The block diagram of overall control scheme with current control using PIR controller is as shown in the Fig. 7.

A. Evaluation of k_p, k_i and k_r values

Considering only the PFC operation, I_{aa} is

$$I_{aa} = \frac{v_{ao} - m_a\frac{V_{dc}}{2}}{r + sL} \tag{8}$$

The forward path gain is given by,

$$\left(k_p + \frac{2k_r\omega_c s}{s^2 + 2\omega_c s + \omega_o^2}\right) * \frac{1}{r + sL} \tag{9}$$

At the cross over frequency $s = \omega_{cross}$ and considering $\omega_{cross} >> \omega_o$ the PR controller transfer function will be similar to the PI [11].

$$G_{PI}(s) = k_{pI}\left(\frac{1 + sT}{sT}\right) \tag{10}$$

The parameters of the PR controller will be determined in the similar way as that of a PI controller. By pole-zero cancellation, $T = \frac{L}{r}$ and k_{pI} will be chosen based on the required bandwidth (ω_{bw}). Choosing ω_{bw} =0.1 (switching frequency), the k_{pI} can be derived as

$$k_{pI} = k_p = \omega_{bw} rT$$

$$k_r = \frac{k_{pI}}{T} = \omega_{bw} r.$$

The parameter $'k_i'$ will depend upon the zero sequence transfer function.

1) The Zero Sequence Network: With PS-SPWM, the zero sequence network can function as a current controlled three phase interleaved dc-dc boost converter along with the PWM rectifier. The per phase current loop of the interleaved dc-dc boost converter is shown in the Fig. 8 By approximating the loop as

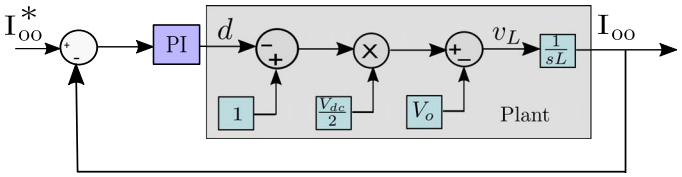

Fig. 8. Per phase block diagram of current controlled boost converter

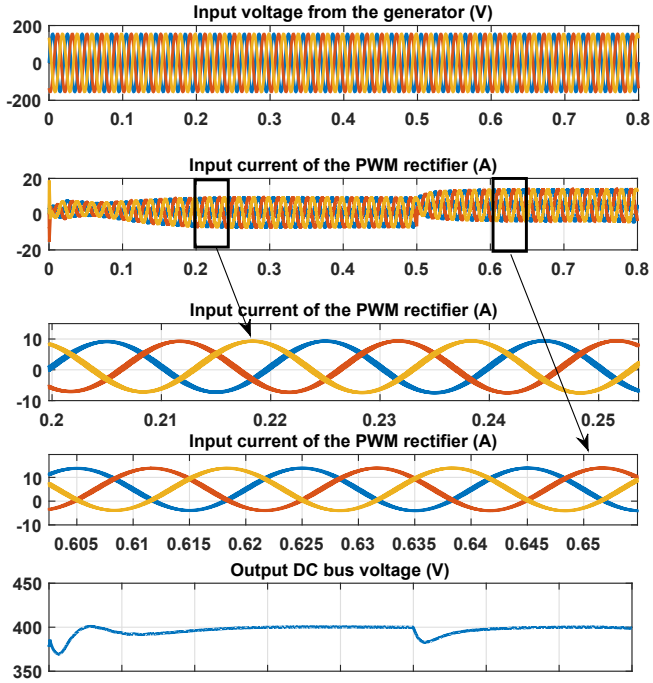

Fig. 9. Performance of the converter with battery in discharging mode

$$\hat{v_L} = V_o d \tag{11}$$

Let the transfer function of the PI controller for the zero sequence current be,

$$G_o(s) = k_o\left(\frac{1 + sT_o}{sT_o}\right) \tag{12}$$

978-1-5386-4536-9/18/$31.00 © 2018 IEEE

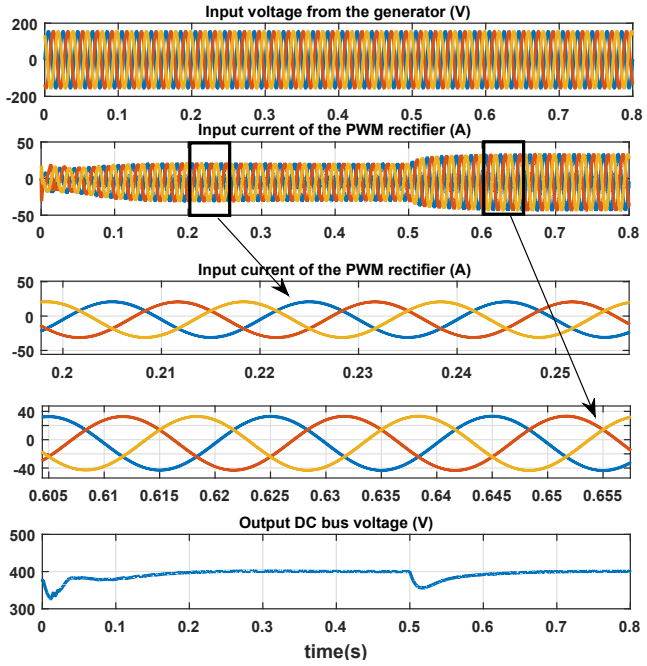

Fig. 10. Performance of the converter with battery in charging mode

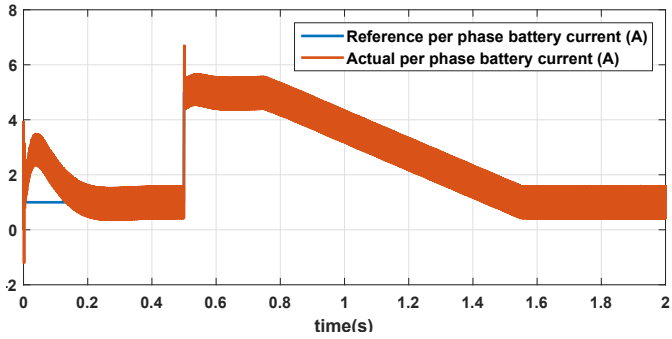

Fig. 11. Per phase battery discharging current

From Fig.8, the closed loop transfer function for the zero sequence network is derived as

$$\frac{I_{oo}}{I^*_{oo}} = \frac{\frac{k_o 0.5 V_{dc}}{T_o L}\left(1 + sT_o\right)}{s^2 + \frac{k_o 0.5 V_{dc}}{L}s + \frac{k_o 0.5 V_{dc}}{T_o L}} \tag{13}$$

Comparing the denominator with that of the second order standard transfer function, the parameter k_i can be determined; $k_i = \frac{k_o}{T_o}$

V. Simulation Results

The three phase PWM rectifier with battery connected to the stator neutral of an Induction Machine is simulated in MATLAB/SIMULINK using the parameters given in Table I.

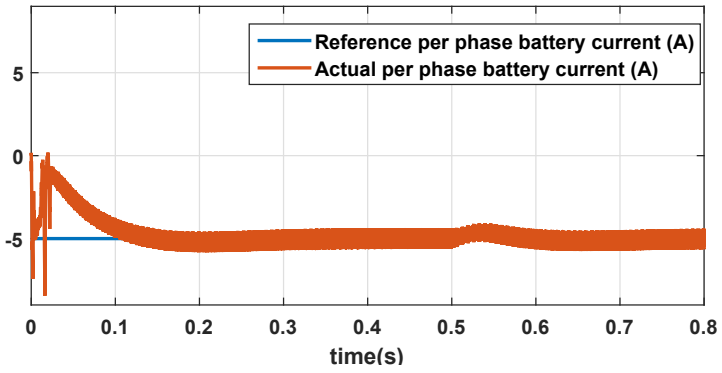

Fig. 12. Per phase battery charging current

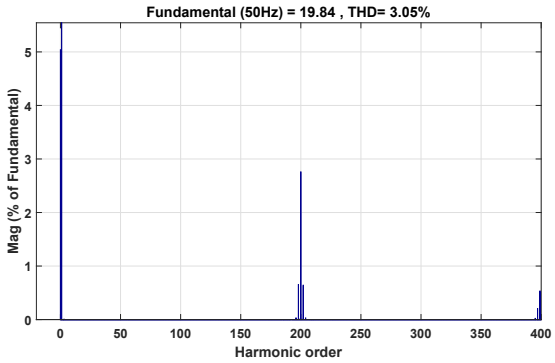

Fig. 13. Harmonic spectrum for I_a

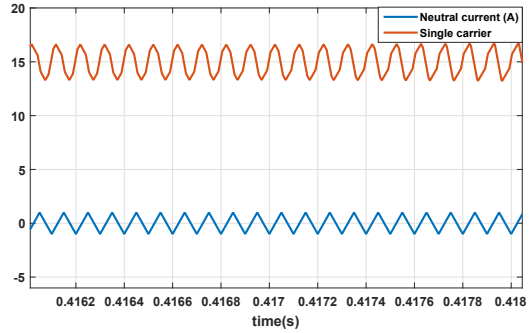

Fig. 14. Ripple current with SPWM

A. Mode I: Battery in discharging mode

Fig. 9 shows the performance of the converter with battery in discharging mode. At time t = 0; battery discharge current reference is set to be 1 A. The generator and the battery together feed a load of 2.5 kW. At time t = 0.5 s, the load is increased from 2.5 kW to 5 kW, and simultaneously the battery current reference is shifted to 5 A, thus improving the transient on the dc bus. After a duration of 2.5 s, the battery current is reduced back to 1 A with a constant negative ramp.

978-1-5386-4536-9/18/$31.00 © 2018 IEEE

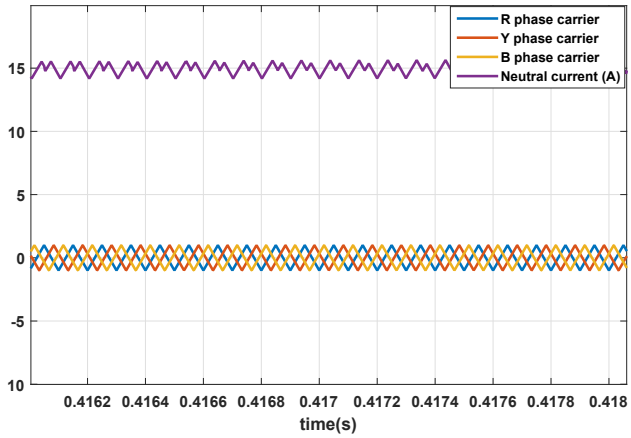

Fig. 15. Ripple current with PS-SPWM

TABLE I: SIMULATION PARAMETERS			
S.No.	**Parameters**	**Symbol**	**value**
1	Rated system capacity	P_{Load}	5 kW
2	Per phase resistance	r	0.1 Ω
3	Per phase leakage inductance	L	5 mH
4	DC bus capacitance	C	1000 μF
5	Per phase generator output voltage	$(V_{ao}, V_{bo} and\ V_{co})$	110 V(RMS)
6	Battery float voltage	V_o	200 V
7	Output DC voltage	V_{dc}	400 V

B. Mode II: Battery in charging mode

Fig. 10 shows the performance of the converter with battery in discharging mode. At time t = 0; the battery discharge current reference is set to 5 A. The generator feeds the load of 2.5 kW and the battery at the same time. At time t = 0.5 s, the load is increased from 2.5 kW to 5 kW; while keeping the battery charging current at the same level.

C. Line current THD

Fig. 13 shows FFT spectrum for the line current I_a. It is observed that with single carrier and phase shifted carrier, the line current THD remains the same.

D. Battery current ripple

Figs. 14 and 15 show the ripple in the total battery current (I_o) in the neutral with single carrier modulation and phase shifted carrier modulation. The battery current reference of 5 A is given to each phase and the total neutral current (I_o) = 15 A. It is observed that for this reference current there is a net reduction of 62.8% in the ripple due to PS-SPWM.

VI. Conclusion

Unified converters have the potential to reduce the size and weight and thereby improve the ergonomics of electric vehicles. A novel topology of integrating battery without the need of a seperate converter for the automotive generator is proposed. The performance of the proposed topology and the control scheme is confirmed through simulation study using MATLAB/SIMULINK package.

References

[1] H. S. Das, C. W. Tan, and A. Yatim, "Fuel cell hybrid electric vehicles: A review on power conditioning units and topologies," *Renewable and Sustainable Energy Reviews*, vol. 76, pp. 268 – 291, 2017.

[2] A. Emadi, S. S. Williamson, and A. Khaligh, "Power electronics intensive solutions for advanced electric, hybrid electric, and fuel cell vehicular power systems," *IEEE Transactions on Power Electronics*, vol. 21, no. 3, pp. 567–577, May 2006.

[3] E. Tazelaar, B. Veenhuizen, J. Jagerman, and T. Faassen, "Energy management strategies for fuel cell hybrid vehicles; an overview," in *2013 World Electric Vehicle Symposium and Exhibition (EVS27)*, Nov 2013, pp. 1–12.

[4] G. T. Chiang and J. i. Itoh, "Dc/dc boost converter functionality in a three-phase indirect matrix converter," *IEEE Transactions on Power Electronics*, vol. 26, no. 5, pp. 1599–1607, May 2011.

[5] J. I. Itoh and D. Ikarashi, "Investigation of a two-stage boost converter using the neutral point of a motor," *IEEE Transactions on Industry Applications*, vol. 49, no. 3, pp. 1392–1399, May 2013.

[6] K. Moriya, H. Nakai, Y. Inaguma, H. Ohtani, and S. Sasaki, "A novel multi-functional converter system equipped with input voltage regulation and current ripple suppression," in *Fourtieth IAS Annual Meeting. Conference Record of the 2005 Industry Applications Conference, 2005.*, vol. 3, Oct 2005, pp. 1636–1642 Vol. 3.

[7] P. Wood, *Switching power converters*, 1981.

[8] R. Teodorescu, F. Blaabjerg, M. Liserre, and P. C. Loh, "Proportional-resonant controllers and filters for grid-connected voltage-source converters," *IEE Proceedings - Electric Power Applications*, vol. 153, no. 5, pp. 750–762, September 2006.

[9] D. N. Zmood and D. G. Holmes, "Stationary frame current regulation of pwm inverters with zero steady-state error," *IEEE Transactions on Power Electronics*, vol. 18, no. 3, pp. 814–822, May 2003.

[10] Q. Yan, X. Wu, X. Yuan, Y. Geng, and Q. Zhang, "Minimization of the dc component in transformerless three-phase grid-connected photovoltaic inverters," *IEEE Transactions on Power Electronics*, vol. 30, no. 7, pp. 3984–3997, July 2015.

[11] B. McGrath, "Principles and practices of digital current regulation for ac systems," Professional Education Seminar Lecture, 2015.

978-1-5386-4536-9/18/$31.00 © 2018 IEEE